Structural characterization of *Alpiniae oxyphyllae* fructus polysaccharide 2 and its activation effects on RAW264.7 macrophages

Xin Yang, Shiwei Zhou, Hong Li, Jiangwen An, Chengheng Li, Ruigang Zhou, Ling Teng, Yongjian Zhu, Suya Liao, Yuhui Yang, Huricha Chen, Yun Chen [*]

Institute of Traditional South Chinese Veterinary Pharmacology, College of Animal Science and Technology, Hainan University, Haikou 570228, PR China

ARTICLE INFO

ABSTRACT

Polysaccharides are important components of *Alpiniae oxyphyllae* fructus that have been shown to exhibit significant immunomodulatory activity in our previous study. However, whether and how *A. oxyphyllae* fructus polysaccharides (AOFP) affect macrophages has not been determined. To further study the immunomodulatory activity of AOFP, the effect of AOFP on RAW264.7 cell activation was investigated in the present work. The results showed that AOFP2 significantly increased the phagocytic activity of RAW264.7 macrophages. AOFP2 promoted the secretion of TNF-α, IL-6, IL-10, TGF-β, NO and iNOS and enhanced the Th2-type immune response via its activation effect on macrophages. Additionally, the structure of AOFP2 was characterized in the present study, as the structural features of polysaccharides determine their biological activities. AOFP2 was only composed of glucose, exhibiting an average molecular weight of 44.3 kDa. Furthermore, the infrared spectroscopy, methylation and nuclear magnetic resonance results indicated that AOFP2 consisted of → 4)-α-D-Glc$p$-(1→, →4,6)-α-D-Glc$p$-(1 → and T-α-Glc$p$.

1. Introduction

Alpiniae oxyphyllae fructus is the dried and mature fruit of *A. oxyphylla* Miq. and is well-known as one of the four traditional southern Chinese medicines. In China, *A. oxyphyllae* fructus is used to treat diarrhea, emesis, frequent urination, and spermatorrhea [1]. Recent studies have indicated that various extracts of *A. oxyphyllae* fructus possess many kinds of biological functions. It has been reported that the ethanol extract of *A. oxyphyllae* fructus has a protective effect on the nervous system, and this extract has been shown to significantly reduce the apoptosis of cortical neurons in mice [2]. Furthermore, the ethanol extract of *A. oxyphyllae* fructus also inhibits the proliferation of human liver cancer cells [3]. Additionally, the methanol extract exerts a positive inotropic effect by inhibiting the sodium and potassium pumps in the myocardium [4].

Polysaccharides, as natural polymers with complex structures, are among the main components of many materials, such as plants, fungi, algae and even animals. Polysaccharides often play important roles in the regulation of the immune system [1,5], tumor growth [6], virus multiplication [7], and oxidative balance [8]. Polysaccharides are the main component of *A. oxyphyllae* fructus. The results of a recent study

[9] indicated that *A. oxyphyllae* fructus polysaccharides (AOFP) cured urinary incontinence in rats. In our previous study, we described three kinds of polysaccharides (AOFP1, AOFP2 and AOFP3) and found that AOFP1 exerted a significant immunomodulatory effect on mouse lymphocytes [1].

Similar to lymphocytes, macrophages play important roles in the body's immune system. Many polysaccharides showed positive regulatory effects on macrophages. For example, *Smilax glabra Roxb*. polysaccharides could effectively promote the phagocytic capacities of macrophages [10], and polysaccharides from *Pleurotus citrinopileatus* significantly increased the secretion of TNF, IL-6 and IL-10 by macrophages [11]. Generally, macrophages are divided into M1-type and M2-type macrophages. M1-type macrophages can induce inflammatory responses and then eliminate pathogens. In contrast, M2-type macrophages can reduce inflammation and then promote tissue repair. We were interested in whether polysaccharides could promote the activation of M1-type macrophages, M2-type macrophages or both and whether AOFP could affect macrophages. Therefore, the effect of AOFP on macrophages was investigated in the present work.

To evaluate the effect of AOFP on macrophages, the viability of RAW264.7 mouse macrophages was determined by MTT assay, and the

---

phagocytic activity of RAW264.7 cells was analyzed by flow cytometry. Additionally, the M1/M2 cytokine levels and Th1/Th2 immune responses were examined by ELISA. As the structural features of polysaccharides determine their physical and physiological properties [12], the chemical structure of the polysaccharides was measured by gel permeation chromatography (GPC)-RI-MALS, high-performance anion exchange chromatography (HPAEC)-PAD, infrared spectroscopy (FT-IR), methylation analysis, and nuclear magnetic resonance (NMR).

2. Materials and methods

2.1. Reagents and materials

A. oxyphyllae fructus was purchased from Lvfuxian Agricultural Development Co., Ltd. (Danzhou, China). Dulbecco's modified Eagle's medium (DMEM) and fetal bovine serum (FBS) were purchased from Gibco Life Technologies (Carlsbad, USA). Penicillin and streptomycin were purchased from HyClone (Logan, USA). All standard monosaccharides (fucose, arabinose, galactose, glucose, xylose, mannose, fructose, ribose, galacturonic acid and glucuronic acid), red blood cell lysis buffer, 3-(4,5-dimethylthiazol-2-yl)-2,5-diphenyltetrazolium bromide (MTT), lipopolysaccharide (LPS), and acetic anhydride were purchased from Sigma-Aldrich (St. Louis, USA). Recombinant murine interleukin-4 (IL-4), the NO assay kit, the inducible nitric oxide synthase (iNOS) assay kit and the enzyme-linked immunosorbent assay (ELISA) kits for mouse IL-2, IL-4, IL-6, IL-10, TNF-α, and IFN-γ were purchased from Beyotime Institute of Biotechnology Co., Ltd. (Shanghai, China). The BCA protein measurement kit was purchased from Nanjing Jiancheng Institute of Biotechnology (Nanjing, China). The Vybrant Phagocytosis Assay Kit (V-6694) was obtained from Thermo Fisher Scientific (Waltham, USA).

2.2. Cells and polysaccharides

The mouse macrophage cell line RAW264.7 was purchased from the Cell Bank of the Chinese Academy of Science (Shanghai, China) and cultured in DMEM supplemented with 10% (V/V) FBS, 100 IU/mL penicillin, 100 IU/mL streptomycin, and 2 mM L-glutamine.

AOFP1, AOFP2 and AOFP3 were prepared as previously described [1]. In brief, crude polysaccharides were extracted by water extraction and the alcohol precipitation method. The proteins in crude polysaccharides were removed by the Sevage method. Then, crude polysaccharides were purified by a DEAE-52 cellulose column and a Sephadex G-100 column. Finally, the purified polysaccharide fractions were collected, dialyzed, concentrated, and freeze-dried.

2.3. Characterization of the polysaccharides

2.3.1. Monosaccharide composition

The monosaccharide composition of AOFP2 was determined according to a previously reported method with some modifications [1]. In brief, the polysaccharide fraction (5 mg) was hydrolyzed in TFA (2 M, 1 mL) at 121 °C for 2 h. Excess TFA was removed by a thermovap sample concentrator. Then, the residue was redissolved in ultrapure water and transferred to a chromatographic flask for analysis. The monosaccharide composition of the polysaccharide fraction was analyzed with an HPAEC (Sunnyvale, USA) equipped with a Dionex™ CarboPac™ PA10 analytical column (250 × 4 mm, 10 μm) with pulsed amperometric detection (PAD).

Fucose, arabinose, galactose, glucose, xylose, mannose, fructose, ribose, rhamnose, galacturonic acid, glucuronic acid and mannuronic acid (100 mg each) were successively added to sterile water and quantitatively dissolved in a 10-mL volumetric flask to prepare a mixed standard solution. The 10 mg/mL standard solution was diluted 100-fold to prepare a 100 μg/mL working solution. Then, the standard working solutions were serially diluted to 1/100, 2/100, 5/100, 10/100, 15/100,

20/100, 25/100 and 30/100. Finally, the diluted solutions were transferred to chromatographic bottles for analysis.

The test polysaccharide fractions and mixed standard solutions were eluted by a gradient of mobile phases: (A) distilled H_2O and (B) 100 mM NaOH (A:B was 97.5:2.5 from 0 to 60 min) with an injection volume of 20 μL.

2.3.2. Molecular weight determination

Dried AOFP2 (5 mg) was dissolved in 0.1 M $NaNO_3$ (1 mL). After centrifugation (14000 rpm, 10 min), the supernatant was collected. The average molecular weight of AOFP2 was measured by gel permeation chromatography with a refractive index (RI) detector and multiangle laser scattering analysis (MALS) (DAWN HELEOS II, USA). Finally, the polysaccharide molecular weights were determined with ASTRA 6.1 software.

2.3.3. FT-IR analysis

The functional groups of AOFP2 were determined by the KBr pressed-tablet method in the range of 400–4000 cm^{-1} [1]. In brief, dried AOFP2 (2 mg) was ground with Kbr powder, pressed into a tablet, and analyzed with a Bruker Tensor 27 FT-IR spectrometer (Karlsruhe, Germany).

2.3.4. Methylation analysis

A dried AOFP2 sample (1 mg) was dissolved in DMSO (500 μL). Then, the polysaccharide solution was mixed with 50 μL of DMSO/NaOH and incubated for 30 min. Next, iodomethane solution (10 μL) was added to the polysaccharide solution and reacted for 10 min. This process was repeated three times, and the reaction time of the third process was 1 h. Then, the polysaccharide solution was mixed with 1 mL distilled water and 500 μL dichloromethane. After the mixture was centrifuged, the water phase was discarded, and the dichloromethane phase was dried and then reacted with TFA (2 M, 100 μL) at 121 °C for 90 min. After the TFA was dried, the sample was mixed with 50 μL of ammonium hydroxide (2 M) and 50 μL of NaBD4 (1 M) at room temperature. After 2.5 h, the reaction was terminated with 20 μL acetic acid, and the sample was dried and then washed twice with 250 μL methanol using a thermovap sample concentrator. Then, the sample was reacted with 250 μL of acetic anhydride for 2.5 h (100 °C). Then, 1 mL of water was added to the sample. Ten minutes later, the sample was mixed with 500 μL dichloromethane. After the mixture was centrifuged, the water phase was discarded, and the dichloromethane phase was obtained for the next detection.

GC–MS was performed by using an Agilent 7820A (Agilent Technologies, USA) GC- system connected with an Agilent 5977B quadrupole mass spectrometry detection system (Agilent Technologies, USA). The GC system was equipped with a BPX70 capillary column (30 m × 0.25 mm × 0.25 μm), and high purity helium (1.0 mL/min) was used as the carrier gas with an injection volume of 1 μL and a split ratio of 10:1. The inlet temperature program was set to 140 °C for 2 min, and then was increased to 230 °C at 3 °C/min for 3 min. Furthermore, the mass spectrometry system was equipped with an electron bombardment ion source and MassHunter workstation, and the ion source was used to detect the analyte in full scan (SCAN) mode. Mass spectrometry analysis was performed at an inlet temperature of 230 °C and a quadrupole temperature of 150 °C, and the scan mode was SCAN with a range (M/Z) from 30 to 600.

2.3.5. NMR analysis

Dried AOFP2 (20 mg) was dissolved in D_2O (0.5 mL) and then placed in a nuclear magnetic tube. Then, the ^1H, ^{13}C, $^1H–^1H$ COSY, HSQC and HMBC NMR spectra were determined by a Bruker AVANCE HD III 600 MHz spectrometer (Karlsruhe, Germany) at 25 °C. The experimental results were obtained using MestReNova 12.0.0 software analysis.

2.4. Cell viability assay

The effects of AOFP1, AOFP2 and AOFP3 on RAW264.7 macrophage viability were determined by MTT assay [10]. First, 100 μL (1×10^5/ mL) RAW264.7 macrophages were seeded into each well of the 96-well plates. Six hours later, the culture medium was replaced with 100 μL of various concentrations of AOFP1, AOFP2, and AOFP3 (39.06–10000 μg/ mL) or DMEM (cell control). After incubation for 24 h, MTT was added to each well of the 96-well plates to a final concentration of 0.5 mg/mL. Four hours later, the supernatant was removed, and DMSO (100 μL) was added to the wells to dissolve the crystallized formazan. The absorbance value of each well was detected by a microplate reader at 570 nm. Finally, RAW264.7 macrophage cell viability was calculated by the ratio of the absorbance value of polysaccharides to the absorbance value of polysaccharides of the control cell.

2.5. Phagocytic activity assay

Based on the results of the cell viability experiment described above, three concentrations (400, 100 and 25 μg/mL) of the polysaccharides were selected to perform the phagocytic activity experiment. The phagocytic activity of macrophages was determined with the Vybrant™ Phagocytosis Assay Kit (V-6694). RAW264.7 macrophages were cultured in 24-well plates for 6 h and then washed three times with PBS. Next, 400 μL of AOFP1, AOFP2 or AOFP3 was added to the poly-saccharide groups, 400 μL of LPS (1 μg/mL) was added to the LPS group, and 400 μL of DMEM was added to the control group. After incubation for 24 h, the supernatant was removed, and the cells were treated with FITC-labeled *Escherichia coli* for 1 h. To remove the excessive *E. coli* particles, the macrophages were washed twice with PBS. Then, 100 μL of trypan blue was added to each well of the 24-well plates and incubated for 1 min at room temperature. Finally, the cells were collected, and the phagocytic activity of the macrophages was measured with a BD FACSCalibur flow cytometer (Bedford, USA) [13].

2.6. Activation effect of AOFP2 on M1-type macrophages

2.6.1. Effect of AOFP2 on IL-6, TNF-α, NO and iNOS secretion by RAW264.7 cells

RAW264.7 macrophages were seeded into 24-well plates. After in-cubation for 6 h, the culture supernatant was replaced with 400 μL of AOFP2 (400, 100 and 25 μg/mL), LPS (1 μg/mL) or DMEM. After in-cubation for 24 h, the levels of IL-6 and TNF-α in the supernatant were measured by mouse IL-6 and TNF-α ELISA kits, respectively. The NO level in the supernatant was determined by the Griess method using an NO assay kit. In addition, the iNOS enzymatic activity was assessed by an iNOS assay kit after the macrophages were lysed with an Ultrasonic Cell Disruptor [14].

2.6.2. Effect of AOFP2-treated RAW264.7 cells on the Th1 immune response

RAW264.7 macrophage cells were cultured in 24-well plates and treated with 400 μL of AOFP2 (400, 100 and 25 μg/mL), LPS (1 μg/mL) or DMEM for 6 h. Then, the culture supernatant was replaced with DMEM. After incubation for 24 h, the supernatant was collected after centrifugation. Lymphocytes were isolated from murine spleens ac-cording to a previously reported method [1] and cultured with the abovementioned supernatant for 24 h. Then, the levels of IL-2 and IFN-γ in the supernatant were determined with mouse IL-2 and IFN-γ ELISA kits, respectively.

2.7. Activation effect of AOFP2 on M2-type macrophages

2.7.1. Effect of AOFP2 on IL-10 and TGF-β secretion by RAW264.7 cells

The RAW264.7 macrophage cell supernatant was collected accord-ing to the method described in Section 2.5.1, except that LPS was replaced with IL-4 (20 ng/mL). The levels of IL-10 and TGF-β in the supernatant were measured by mouse IL-10 and TGF-β ELISA kits.

2.7.2. Effect of AOFP2-treated RAW264.7 cells on the Th2 immune response

RAW264.7 macrophage cells were seeded in 24-well plates, treated with 400 μL of AOFP2 (400, 100 and 25 μg/mL), IL-4 (20 ng/mL) or DMEM for 6 h and then treated with DMEM for 24 h. The supernatant was collected. To accurately evaluate the effect of the supernatant on lymphocytes, the IL-4 and IL-6 levels in the supernatant were deter-mined by mouse IL-4 and IL-6 ELISA kits, respectively. In addition, lymphocytes from murine spleens were treated with the above-mentioned supernatant for 24 h, and the IL-4 and IL-6 levels were determined.

2.8. Statistical analysis

All the results are expressed as the mean ± SD from three indepen-dent experiments. The statistical analyses were performed by Duncan's multiple range test. All statistical analyses were performed using SPSS 20.0 software.

3. Results

3.1. Effect of AOFP on RAW264.7 cell viability

Fig. 1 shows the effects of AOFP1, AOFP2 and AOFP3 on RAW264.7 macrophage cell viability. All three polysaccharides exhibited cytotox-icity on RAW264.7 cells when their action concentrations were 10000 μg/mL. Clearly, AOFP1 and AOFP3 had no toxic effects on macrophages when the concentrations were lower than 5000 μg/mL. Furthermore, RAW264.7 cell viability was promoted by AOFP1 and AOFP3 in a concentration-dependent manner at concentrations ranging from 39.06 μg/mL to 5000 μg/mL. Although the cell viability under AOFP2 treat-ment at 5000 μg/mL was higher than that of the cell control (100%), it was lower than that of AOFP2 at 2500 μg/mL. Furthermore, AOFP2 showed a promoting effect on RAW264.7 cell viability in a concentration-dependent manner at concentrations ranging from 39.06 μg/mL to 2500 μg/mL. This result indicated that AOFP2 at 5000 μg/mL showed both cytotoxic and promoting effects on macrophages. There-fore, AOFP2 was deemed to have no cytotoxicity when its concentration
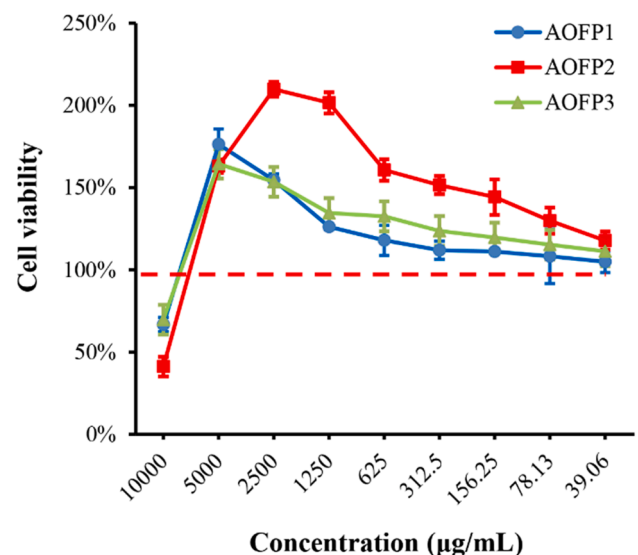

Fig. 1. Cell viability of RAW264.7 cells RAW264.7 cells were treated with DMEM, AOFP1, AOFP2 and AOFP3 for 24 h. After that, the cell viability of each group was tested by MTT method.

was lower than 2500 µg/mL. Of course, it is obvious that the cell viabilities of the AOFP2-treated RAW264.7 macrophage cells were higher than those of AOFP1-treated and AOFP3-treated RAW264.7 macrophage cells. Based on these results, concentrations of 400, 100 and 25 µg/mL were chosen for the subsequent experiments.

3.2. Effect of AOFP on the phagocytic activity of RAW264.7 cells

The phagocytic activities of RAW264.7 cells treated with the three polysaccharides were measured by flow cytometry (Fig. 2). The phagocytic activities of the AOFP1 and AOFP2 groups (400 µg/mL, 100 µg/mL and 25 µg/mL) and the AOFP3 groups (400 µg/mL and 100 µg/mL) were significantly ($P < 0.05$) higher than those of the control group. Additionally, AOFP1, AOFP2 and AOFP3 promoted phagocytosis in a dose-dependent manner. Furthermore, AOFP2 exerted the most significant promoting effect, and the effect of 400 µg/mL AOFP2 was stronger than that of LPS ($P < 0.05$). Therefore, AOFP2 was selected as the research object for the subsequent study.
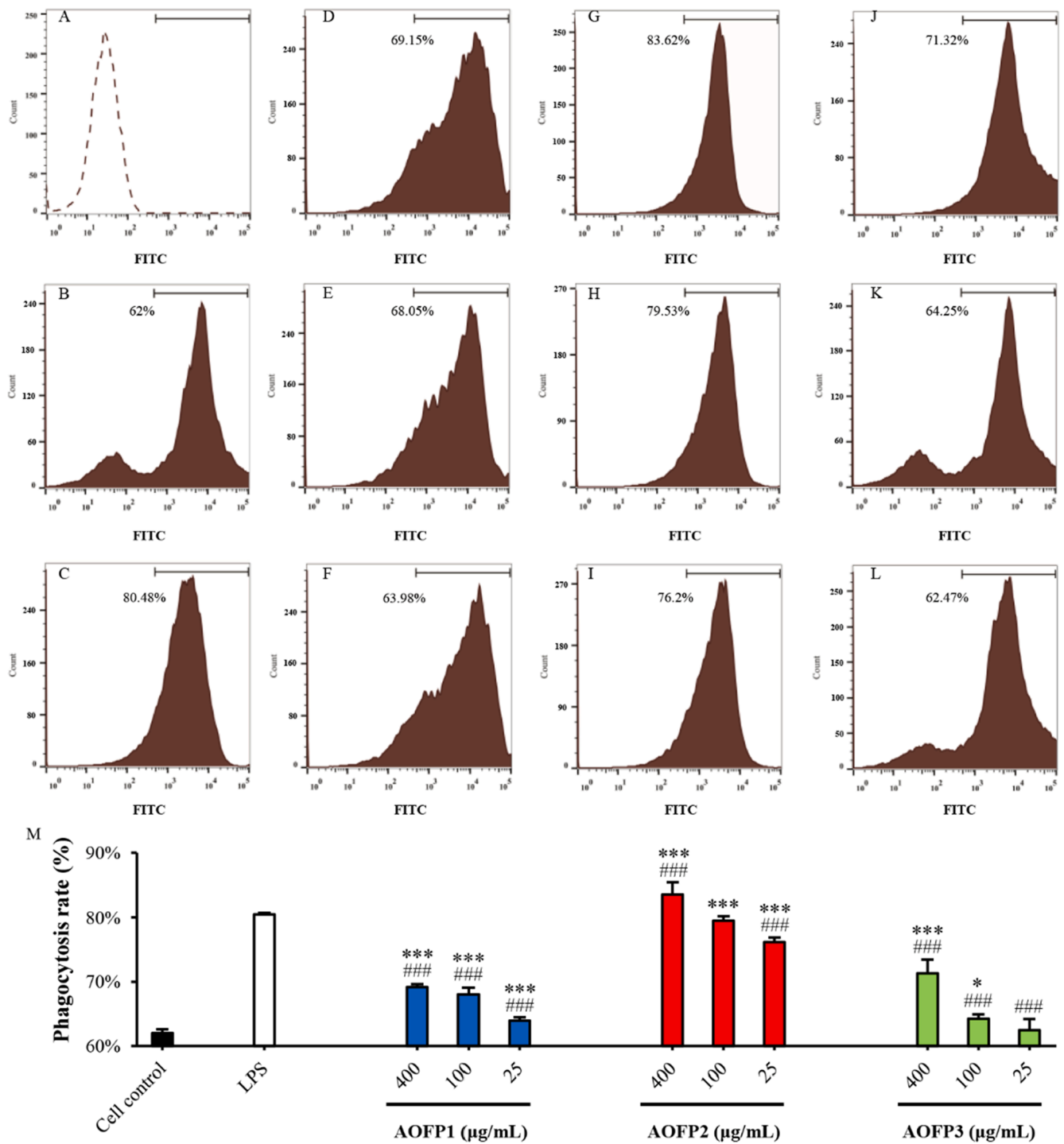

Fig. 2. Effect of AOFP on phagocytic activity of RAW264.7 cells RAW264.7 cells were treated with DMEM (B, as a cell control), LPS (C, 1 µg/mL), AOFP1 (D, 400 µg/mL; E, 100 µg/mL; F, 25 µg/mL), AOFP2 (G, 400 µg/mL; H, 100 µg/mL; I, 25 µg/mL), and AOFP3 (J, 400 µg/mL; K, 100 µg/mL; L, 25 µg/mL) for 24 h. Then the phagocytic activity was tested by using Vybrant Phagocytosis Assay Kit (V-6694). A, blank control; M, statistical data of the results of phagocytosis of RAW264.7 cells. *$p < 0.05$, ***$p < 0.001$ versus cell control group; ###$p < 0.001$ versus LPS group.

3.3. Characterization of AOFP2

3.3.1. Determination of molecular weight and monosaccharide composition

The average molecular weight of AOFP2 was determined by the GPC-RI-MALS method (Fig. 3A). A sharp, single peak was clearly observed in Fig. 3A, proving that AOFP2 was a homogeneous polysaccharide fraction. The average molecular weight of AOFP2 was 44.3 kDa, as determined by detecting the sample signal and calculating the retention time by using a RI-MALS detector. The monosaccharide composition of AOFP2 was determined by HPAEC (Fig. 3C). The results showed that AOFP2 was composed of glucose alone.

3.3.2. FT-IR analysis

The results of infrared analysis of AOFP2 are shown in Fig. 4A. A strong absorption peak was generated due to the tensile vibration of O-H at 3420.79 cm^{-1}. The signal at 2939.18 cm^{-1} was attributed to the C-H tensile vibration. The strong peaks at 1641.41 and 1381.82 cm^{-1} were caused by the tensile vibrations of O-H and C-H [15,16]. These results indicated that AOFP2 displayed characteristic polysaccharide absorption bands. Furthermore, the signals at 854.53 and 762.41 cm^{-1} indicated the presence of α-glycosidic bonds [17,18], and the absorbances at 1024.05 and 1081.18 cm^{-1} were signals of pyranose rings [15]. In addition, the signal at 933.28 cm^{-1} indicated that AOFP2 contained glucose, which verified the results of the monosaccharide composition analysis shown in Fig. 3C [8].

3.3.3. Methylation and NMR analysis

Methylation analysis and NMR were used to identify the exact glycosidic bond types, linkage patterns and configuration of AOFP2. The methylation analysis results (Table 1) showed that AOFP2 contained three glycosidic linkages, including T-α-Glc*p*, →4)-α-D-Glc*p*-(1 → and → 4,6)-α-D-Glc*p*-(1→, with molar percentage ratios of 16.86%, 74.05% and 9.09%, respectively.

In the ^{1}H NMR spectrum (Fig. 4B), three signals (5.41, 5.38 and 4.98 ppm) and D$_2$O solvent (4.80 ppm) peaks were present in the anomeric proton region (4.50–5.50 ppm). Furthermore, various H2-H5 signals were distributed in the nonanomeric proton region (3.40–4.5 ppm). The three anomeric proton chemical shifts at 5.41, 5.38 and 4.98 ppm were assigned to H-1 of three sugar residues. Similarly, the anomeric carbon signals at δ 100.11, 99.60 and 98.58 in the ^{13}C spectrum (Fig. 4C) indicated the C-1 of three sugar residues in AOFP2. According to the HSQC NMR spectrum (Fig. 4D), three cross peaks were observed at 4.98/100.11, 5.38/99.60 and 5.41/98.58 ppm, which verified the H1/C1 signals of the three glycoside bonds. Based on the results of the methylation analysis and the reported data, the signals at 4.98/100.11, 5.38/99.60 and 5.41/98.58 ppm were attributed to → 4,6)-α-D-Glc*p*-(1→, →4)-α-D-Glc*p*-(1 → and T-α-Glc*p*, respectively [19–21].

As shown in the COSY spectrum (Fig. 4E), the cross peaks at 5.38/

3.45, 3.45/3.79, 3.79/3.65, 3.65/4.04 and 4.04/3.28 ppm represented H1/H2, H2/H3, H3/H4, H4/H5 and H5/H6 of → 4)-α-D-Glc*p*-(1→, respectively. This result proved that 3.45, 3.79, 3.65, 4.04 and 3.28 ppm were attributed to H2, H3, H4, H5 and H6 of → 4)-α-D-Glc*p*-(1→, respectively [20]. Similarly, H1/H2, H2/H3, H3/H4, H4/H5 and H5/H6 of → 4,6)-α-D-Glc*p*-(1 → were present at 4.98/3.65, 3.65/3.99, 3.99/3.86, 3.86/4.04 and 4.04/3.67 ppm, indicating that 3.65, 3.99, 3.86, 4.04 and 3.67 ppm were attributed to H2, H3, H4, H5 and H6, respectively [19]. Furthermore, the signals of other protons in T-α-Glc*p* (from H-2 to H-6) were 3.61, 3.67, 3.43, 3.72 and 3.84 ppm for H-2, H-3, H-4, H-5 and H-6, respectively [21]. Based on the COSY and HSQC spectra, the chemical shifts of δ 78.90, 74.89, 72.84, 71.49 and 60.43 were attributed to C2, C3, C4, C5 and C6 of → 4)-α-D-Glc*p*-(1→, respectively. In the same way, the signals of 71.14, 73.32, 76.68 and 69.28 ppm were identified as C2-C5 of → 4,6)-α-D-Glc*p*-(1→, respectively. The cross peaks at 3.61/74.49, 3.67/76.81 and 3.43/72.67 ppm confirmed that 74.49, 76.81 and 72.67 ppm were assigned to C2-C4 of T-α-Glc*p*, respectively.

The glycoside linkage of AOFP2 was deduced by alternating overlapping peaks of the HMBC spectrum. As presented in Fig. 4 F, H-1 of T-α-D-Glc*p*-(1 → was connected to C-4 of → 4)-α-D-Glc*p*-(1 → or C-4 of → 4,6)-α-D-Glcp-(1→, and H-1 of → 4)-α-D-Glc*p*-(1 → was connected to C-4 of → 4)-α-D-Glc*p*-(1 → or C-4 of → 4,6)-α-D-Glc*p*-(1→. In addition, C-1 of → 4)-α-D-Glc*p*-(1 → was connected to H-4 of → 4,6)-α-D-Glc*p*-(1→, and C-1 of T-α-D-Glc*p*-(1 → was connected to H-6 of → 4,6)-α-D-Glc*p*-(1→. Furthermore, C-1 of → 4,6)-α-D-Glc*p*-(1 → was connected to H-4 of → 4)-α-D-Glc*p*-(1 → or H-6 of → 4,6)-α-D-Glc*p*-(1→. Therefore, the main chain of AOFP2 was composed of → 4)-α-D-Glc*p*-(1→, and the terminal group α-D-Glc*p*- (1 → was connected to the main chain by a → 4,6) -α-D-Glc*p*-(1 → bond. The speculated structural formula of AOFP-2 is shown in Fig. 5

3.4. Effect of AOFP2 on M1-type macrophages

Fig. 6 shows the effect of AOFP2 on M1-type macrophages. In response to AOFP2 treatment, the levels of IL-6, TNF-α, NO and iNOS in the RAW264.7 cells were increased in a dose-dependent manner (Fig. 6A-D). The levels in the AOFP2 group were significantly higher than those in the control group. These results indicated that AOFP2 could promote the polarization of M1-type macrophages.

To investigate the effect of AOFP2-treated macrophages on the Th1 immune response, the IL-2 and IFN-γ levels in murine lymphocytes cultured with AOFP2-treated macrophage supernatant were detected. The results showed that there was no significant difference between the IL-2 and IFN-γ contents in the AOFP2 group and those in the control group (*P* > 0.05). AOFP2 (400, 100 and 25 µg/mL) had no effect on the Th1 immune response via its activation on macrophages (Fig. 6E-F).
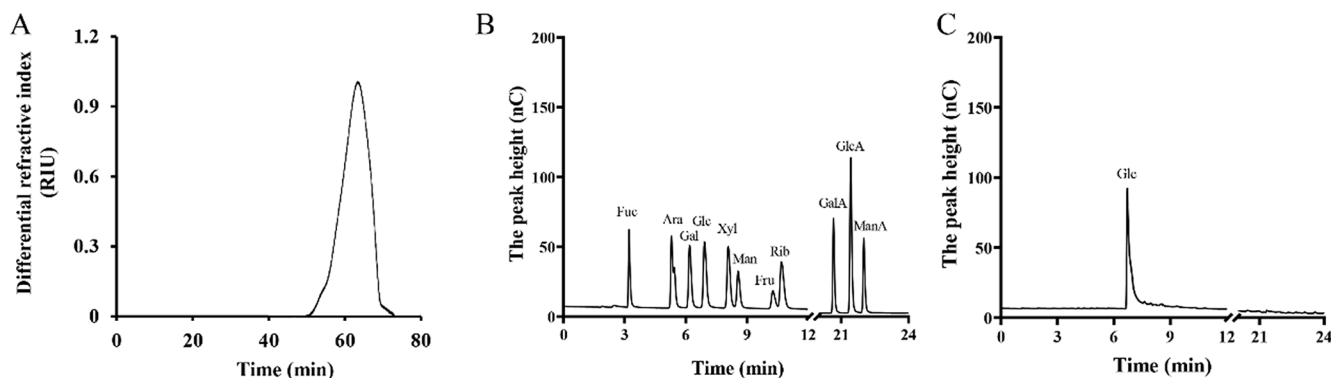

Fig. 3. Molecular weight and monosaccharide composition of AOFP2 A, Molecular weight determination of AOFP2 was determined by GPC chromatography; B, Monosaccharide composition of the polysaccharides was determined by HPAEC-PAD.
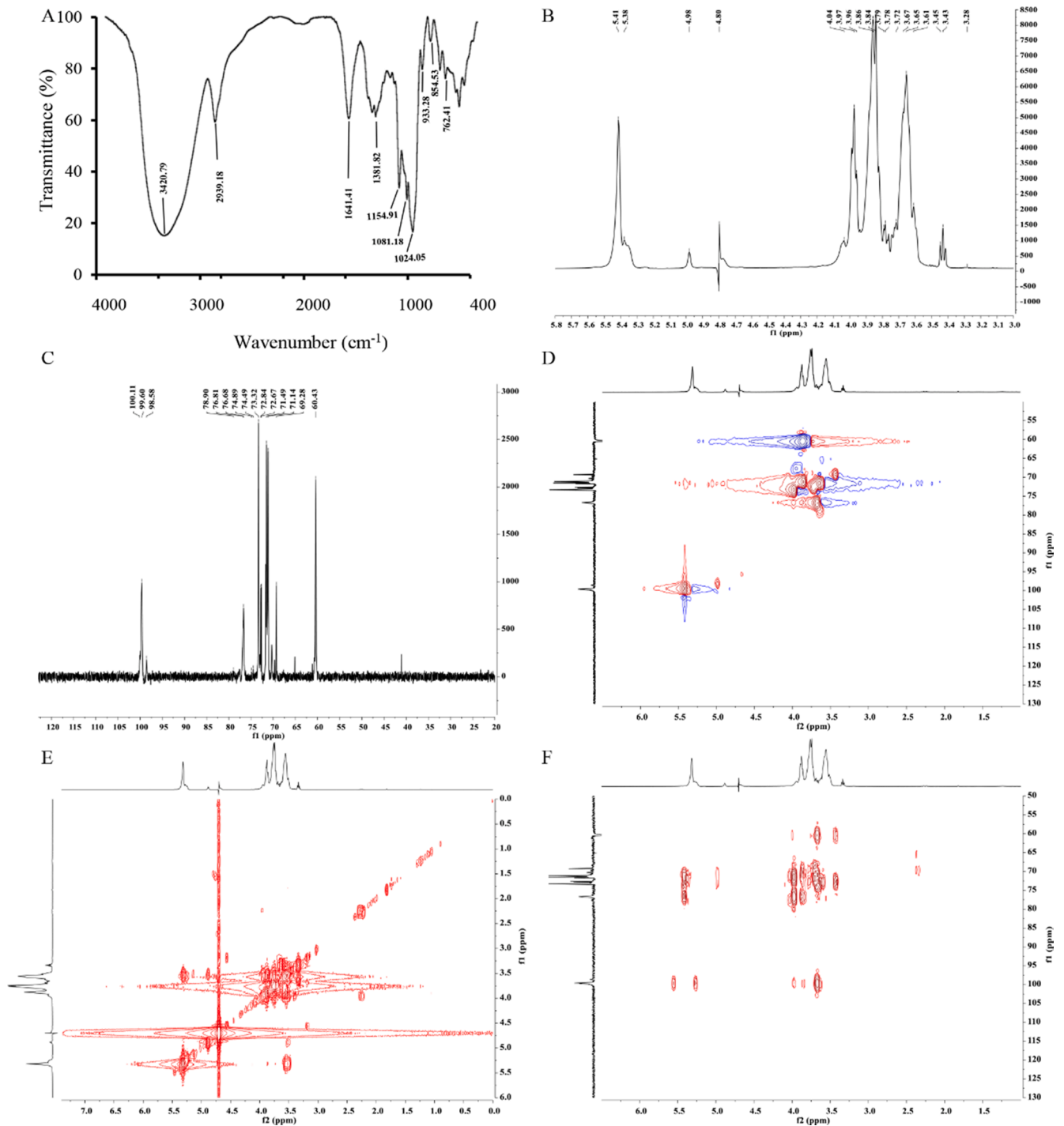
Fig. 4. FT-IR and NMR spectra of AOFP2 The IR spectrum (A) and NMR spectrum (B, ¹H; C, ¹³C; D, HSQC; E, COSY; F, HMBC) were also used to analyze the characterization of the AOFP2.

Table 1
Methylation analysis of AOFP2.

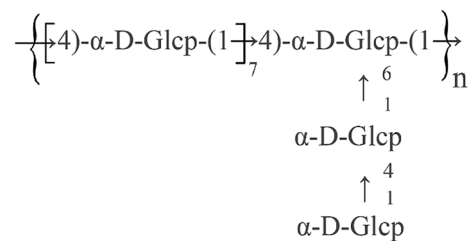| Sugar derivatives	Linkage types	Mole ratio (%)
1,5-di-O-acetyl-2,3,4,6-tetra-O-methyl glucitol	t-Glc(p)	16.86
1,4,5-tri-O-acetyl-2,3,6-tri-O-methyl glucitol	4-Glc(p)	74.05
1,4,5,6-tetra-O-acetyl-2,3-di-O-methyl glucitol	4,6-Glc(p)	9.09

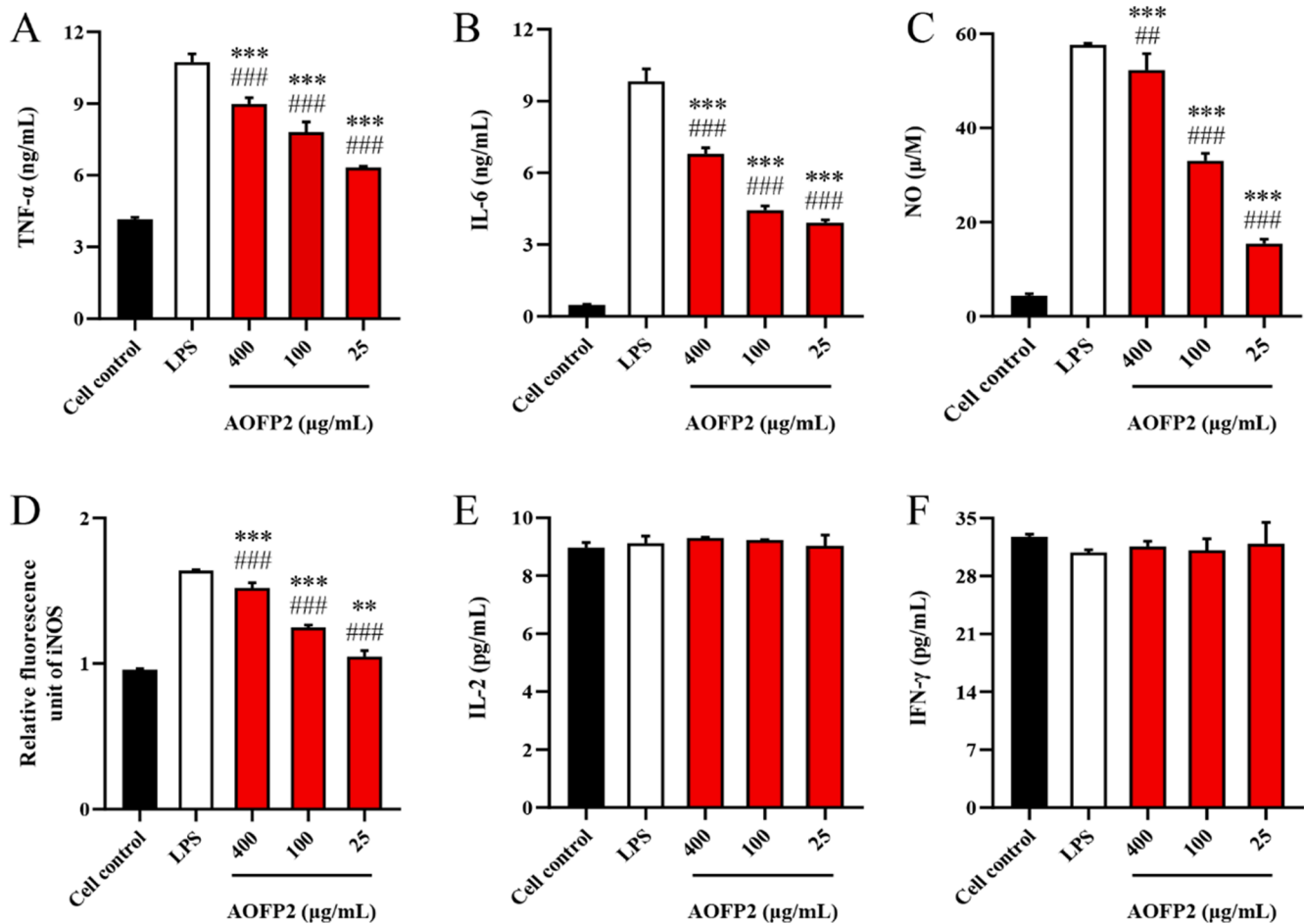**Fig. 5.** Structural formula of AOFP2.

Fig. 6. Effect of AOFP2 on M1 type macrophages RAW264.7 cells were treated with DMEM, LPS (1 μg/mL) and AOFP2 (400 μg/mL, 100 μg/mL, 25 μg/mL) for 24 h. The TNF-α (A), IL-6 (B), NO (C) and iNOS (D) levels in the culture supernatant were tested. RAW264.7 cells were treated with DMEM, LPS (1 μg/mL) and AOFP2 (400 μg/mL, 100 μg/mL, 25 μg/mL) for 6 h and then treated with DMEM for 24 h. The culture supernatant were collected and used to culture mouse spleen lymphocytes. After 24 h, the IL-2 (E) and IFN-γ (F) levels were treated. $**p < 0.01$, $***p < 0.001$ versus cell control group; $^{##}p < 0.01$, $^{###}p < 0.001$ versus LPS group.

3.5. Effect of AOFP2 on M2-type macrophages

The effect of AOFP2 on M2-type macrophages is shown in Fig. 7. AOFP2 promoted IL-10 and TGF-β secretion in a dose-dependent manner (Fig. 7A and B). The IL-10 and TGF-β contents in the AOFP2 group were significantly ($P < 0.05$) higher than those in the control group. Moreover, the IL-10 levels in the AOFP2 groups (400 and 100 μg/mL) were significantly ($P < 0.05$) higher than those in the IL-4 group (Fig. 7A). These findings suggested that AOFP2 promoted the polarization of M2-type macrophages.

Similarly, we also investigated the effect of AOFP2-treated macrophages on the Th2 immune response by measuring the IL-4 and IL-6 levels. As the positive control in the M2-type macrophage assay was IL-4, and AOFP2 promoted RAW264.7 cells to secrete significant amounts of IL-6, RAW264.7 cells were treated with IL-4 and AOFP2 for 6 h and then treated with DMEM for 24 h. The IL-4 and IL-6 levels in the RAW264.7 cells following this treatment were measured. The results showed that the IL-4 levels in each group were the same (Fig. 7C). However, the IL-6 levels in the AOFP2 groups (400 and 100 μg/mL) were significantly higher than those in the control group and IL-4 group (Fig. 7E). Interestingly, when the concentration of AOFP2 was 400 μg/mL, the IL-6 content was 465 pg/mL (Fig. 7E) in the RAW264.7 cell culture supernatant and 1190 pg/mL (Fig. 7F) in the lymphocyte culture supernatant. Furthermore, AOFP2-treated RAW264.7 cells promoted significant amounts of IL-4 secretion by lymphocytes (Fig. 6D). This

result indicated that AOFP2 could induce a Th2-type immune response through its activation of macrophages.

4. Discussion

Macrophages play crucial and distinct roles in the immune system [22]. These cells eliminate invading bacteria, remove senescent and damaged cells, and kill tumor cells. Therefore, the activation of macrophages is an important immunomodulatory biological mechanism. Polysaccharides often possess immunomodulatory activities. Many polysaccharides have been reported to exhibit excellent activation effects on macrophages [5,14,23]. In our previous study, we found that AOFP is an immunomodulator. AOFP1, AOFP2 and AOFP3 significantly promoted the Th1-type and Th2-type immune responses of mouse lymphocytes [1]. In this study, we investigated the effect of AOFP on RAW264.7 cells to further evaluate its immunomodulatory effect.

Natural polysaccharides often show low cytotoxicity. The polysaccharides from *Cyclocarya paliurus*, *Grateloupia livida* (Harv.) Yamada and *Smilax glabra Roxb.* promoted the viability of RAW264.7 cells and showed no cytotoxic effects on the cells at concentrations lower than 400 μg/mL, 256 μg/mL and 500 μg/mL [10,24,25]. Furthermore, *Atractylodis macrocephalae* Rhizoma polysaccharides showed no cytotoxic effects on RAW264.7 cells, even at a concentration of 1 mg/mL [26]. In our previous study, AOFP1, AOFP2 and AOFP3 did not decrease the cell viability of lymphocytes at 8 mg/mL [1]. In the present study,
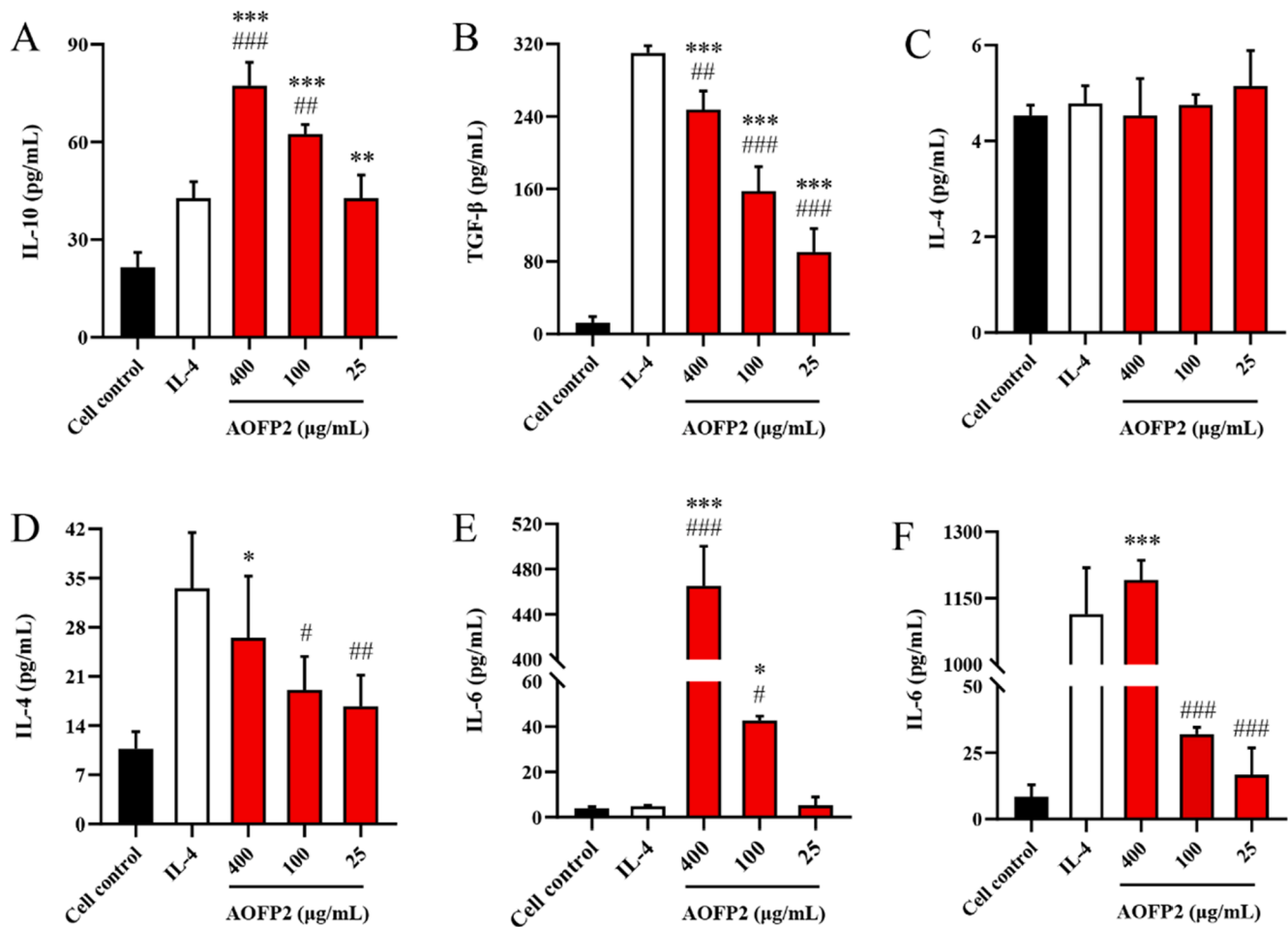
Fig. 7. Effect of AOFP2 on M2 type macrophages RAW264.7 cells were treated with DMEM, IL-4 (20 ng/mL) and AOFP2 (400 μg/mL, 100 μg/mL, 25 μg/mL) for 24 h. The IL-10 (A) and TGF-β (B) levels in the culture supernatant were tested. RAW264.7 cells were treated with DMEM, IL-4 (20 ng/mL) and AOFP2 (400 μg/mL, 100 μg/mL, 25 μg/mL) for 6 h and then treated with DMEM for 24 h. The IL-4 (C) and IL-6 (E) contents in the culture supernatant were tested. Mouse spleen lymphocytes were treated with the abovementioned culture supernatant for 24 h. Afterwards, the IL-4 (D) and IL-6 (F) levels were tested. $*p < 0.05$, $**p < 0.01$, $***p < 0.001$ versus cell control group; $^{\#}p < 0.05$, $^{\#\#}p < 0.01$, $^{\#\#\#}p < 0.001$ versus LPS group.

AOFP1, AOFP2 and AOFP3 promoted the viability of RAW264.7 cells and exhibited no cytotoxic effects at concentrations of 5 mg/mL, 2.5 mg/mL and 5 mg/mL, respectively (Fig. 1). This result indicated that the toxicity of AOFP is extremely low and further verified that polysaccharides are safe drugs.

M1-type and M2-type macrophages are two different types of macrophages that have opposing functions. M1-type macrophages are activated by Th1 cytokines (IFN-γ), microbial products (LPS), and endogenous stress signals (heat shock proteins). This kind of macrophage produces a large number of proinflammatory cytokines (IL-6 and TNF-α) and induces iNOS to produce NO [11,23,27]. The inflammatory response promoted by M1-type macrophages has a strong ability to kill pathogenic microorganisms and germs. However, a side effect of this response is tissue destruction [27]. M2-type macrophages are also known as IL-4/IL-13-induced macrophages. IL-10/TGF-β released by M2-type macrophages has the ability to remodel and repair tissue, promote anti-inflammatory factor secretion, and clear debris [28,29]. Clearly, M2-type macrophages play a key role in reducing inflammation. Therefore, the regulation of the balance between M1-type and M2-type macrophages is important. Furthermore, as polarized macrophages are pivotal for disease progression [23], the regulation of macrophage polarization is important for health. It is well known that many polysaccharides have regulatory effects on macrophage activation, and some studies have also shown that polysaccharides have effects on macrophage polarization. Minato et al. [11] reported that *Pleurotus*

citrinopileatus polysaccharides reduced the secretion of TNF and IL-6 by macrophages and increased the secretion of the anti-inflammatory cytokine IL-10, indicating that polysaccharides lead to polarization of monocytes toward the M2 macrophage subtype. In contrast, another study [23] showed that polysaccharides from *Platycladus orientalis* (L.) Franco leaves increased TNF-α and IL-6 levels in macrophages and decreased TGF-β levels in macrophages. In our present work, we studied the effect of AOFP2 on the activation and polarization of RAW264.7 cells. The results showed that AOFP2 exerted a significant promoting effect on RAW264.7 cell activation (Fig. 2). Furthermore, AOFP2 increased the TNF-α, IL-6, NO, iNOS, IL-10, and TGF-β levels (Figs. 6 and 7). These results indicated that AOFP2 induced RAW264.7 cells to differentiate into both M1-type and M2-type macrophages. Thus, AOFP2 not only exerts a proinflammatory effect to help the host fight pathogens in the early stage of infection but also exerts an anti-inflammatory effect to repair the damaged tissue in the later stage of infection. This observation demonstrated that AOFP2 can promote immune balance in the body. Clearly, there was a substantial difference between the results of our present work and the results of the abovementioned studies on the effects of polysaccharides on macrophage polarization [11,23]. Thus, although most polysaccharides showed a promoting effect on macrophages, the regulatory effects of different polysaccharides on macrophage polarization are diverse. This difference might be due to the various structural features of polysaccharides [12]. The structure of AOFP2 was characterized in the present work (Table 1, Figs. 3 and 4).

The results showed that AOFP2 was a homoglycan consisting of → 4)-α-D-Glc*p*-(1→, →4,6)-α-D-Glc*p*-(1 → and T-α-Glc*p*, with an average molecular weight of 44.3 kDa. AOFP2 was eluted by 0.2 M NaCl solution using a DEAE-52 cellulose column, while AOFP1 was eluted by dH$_2$O [4]. The structures of the two polysaccharides were different. AOFP1 was composed of arabinose, galactose, glucose, xylose, mannose, galacturonic acid and glucuronic acid, while AOFP2 was only composed of glucose. The different structures resulted in the different immunomodulatory activities of the two polysaccharides: AOFP1 exhibited a better promoting effect on lymphocytes [1], and AOFP2 exhibited a better regulatory effect on macrophages (Fig. 2).

The immune system is a complex network. Macrophage polarization is regulated by Th1 and Th2 cytokines. Th1 cytokines, such as IFN-γ, polarize macrophages toward an M1 inflammatory state, while Th2 cytokines, such as IL-4, polarize macrophages toward an M2 phenotype [23,27]. This was also verified in the present work (Figs. 6 and 7). In addition, we also wanted to determine whether AOFP2 had a regulatory effect on Th1-type and Th2-type immune responses via its polarizing effect on macrophages. The results showed that AOFP2 had no effect on the secretion of Th1 cytokines (IFN-γ and IL-2) via its regulatory effect on macrophages (Fig. 6). However, AOFP2 significantly increased Th2 cytokine (IL-4 and IL-6) levels (Fig. 7). Because Th2 cytokines can polarize macrophages toward the M2 phenotype, AOFP2 likely mainly promoted M2-type macrophage polarization *in vivo*. AOFP2 might be used as a drug for tissue repair. Of course, the regulatory effect of AOFP2 on macrophages *in vivo* and the underlying mechanism such as the cell receptor for AOFP3 (TLR2/4) and cell signaling pathways (NF-κB and MAPKs), warrant further study.

5. Conclusion

AOFP1, AOFP2 and AOFP3 all promoted the activation of RAW264.7 cells, and the effect of AOFP2 was the strongest. AOFP2 polarized RAW264.7 cells toward both the M1 and M2 phenotypes. In addition, AOFP2 could enhance the Th2-type immune response via its polarizing effect on macrophages. AOFP2 was composed only of glucose with an average molecular weight of 44.3 kDa. Further structural characterization studies showed that AOFP2 was a homoglycan consisting of → 4)-α-D-Glc*p*-(1→, →4,6)-α-D-Glc*p*-(1 → and T-α-Glc*p*.

Acknowledgment

References

[1] X. Yang, Y.H. Yang, H. Chen, T. Xu, C.H. Li, R.G. Zhou, L.L. Gao, M.M. Han, X.T. He, Y. Chen, Extraction, isolation, immunoregulatory activity, and characterization of Alpiniae oxyphyllae fructus polysaccharides, Int. J. Biol. Macromol. 155 (2020) 927–937.

[2] X.Y. Yu, L.J. An, Y.Q. Wang, H. Zhao, C.Z. Gao, Neuroprotective effect of Alpinia oxyphylla Miq. fruits against glutamate-induced apoptosis in cortical neurons, Toxicol. Lett. 144 (2003) 205–212.

[3] Z.H. He, W. Ge, G.G. Yue, C.B. Lau, M.F. He, P.P. But, Anti-angiogenic effects of the fruit of Alpinia oxyphylla, J. Ethnopharmacol. 132 (2010) 443–449.

[4] N. Shoji, A. Umeyama, Y. Asakawa, T. Takemoto, K. Nomoto, Y. Ohizumi, Structural determination of nootkatol, a new sesquiterpene isolated from Alpinia oxyphylla Miquel possessing calcium-antagonistic activity, J. Pharm. Sci. 73 (1984) 543–544.

[5] Y. Rong, R.L. Yang, Y.Z. Yang, Y.Z. Wen, S.X. Liu, C.F. Li, Structural characterization of an active polysaccharide of longan and evaluation of immunological activity, Carbohyd. Polym. 213 (2019) 247–256.

[6] W.F. Li, X.Y. Hu, S.P. Wang, Z.R. Jiao, T.Y. Sun, T.Q. Liu, K.D. Song, Characterization and anti-tumor bioactivity of astragalus polysaccharides by immunomodulation, Int. J. Biol. Macromol. 145 (2020) 985–997.

[7] L.C. Faccin-Galhardi, K.A. Yamamoto, S. Ray, B. Ray, R.E.C. Linhares, C. Nozawa, The in vitro antiviral property of Azadirachta indica polysaccharides for poliovirus, J. Ethnopharmacol. 142 (2012) 86–90.

[8] R.G. Zhu, X.Y. Zhang, Y. Wang, L.J. Zhang, J. Zhao, G. Chen, J.G. Fan, Y.F. Jia, F.W. Yan, N. Chong, Characterization of polysaccharide fractions from fruit of Actinidia arguta and assessment of their antioxidant and antiglycated activities, Carbohyd. Polym. 210 (2019) 73–84.

[9] Y. Han, J. Wu, Y.S. Liu, J.L. Qi, C. Wang, T. Yu, Y.L. Xia, H.L. Li, Therapeutic effect and mechanism of polysaccharide from Alpiniae oxyphyllae fructus on urinary incontinence, Int. J. Biol. Macromol. 128 (2019) 804–813.

[10] M. Wang, X.B. Yang, J.W. Zhao, C.J. Lu, W. Zhu, Structural characterization and macrophage immunomodulatory activity of a novel polysaccharide from Smilax glabra Roxb, Carbohyd. Polym. 156 (2017) 390–402.

[11] K.I. Minato, L.C. Laan, I.V. Die, M. Mizuno, Pleurotus citrinopileatus polysaccharide stimulates anti-inflammatory properties during monocyte-to-macrophage differentiation, Int. J. Biol. Macromol. 122 (2019) 705–712.

[12] S.S. Ferreira, C.P. Passos, P. Madureira, M. Vilanova, M.A. Coimbra, Structure-function relationships of immunostimulatory polysaccharides: a review, Carbohyd. Polym. 132 (2015) 378–396.

[13] S.J. Liu, D.M. Boeck, H.V. van Dam, T.P. Dijke, Regulation of the TGF-β pathway by deubiquitinases in cancer, Int. J. Biochem. Cell B. 76 (2016) 135–145.

[14] W.J. Sun, W.J. Hu, K. Meng, L.M. Yang, W.M. Zhang, X.P. Song, X.H. Qu, Y.Y. Zhang, L. Ma, Y.P. Fan, et al., Activation of macrophages by the ophiopogon polysaccharide liposome from the root tuber of Ophiopogon japonicas, Int. J. Biol. Macromol. 91 (2016) 918–925.

[15] J.X. Song, Y. Wu, X.J. Ma, L.J. Feng, Z.G. Wang, G.Q. Jiang, H.B. Tong, Structural characterization and α-glycosidase inhibitory activity of a novel polysaccharide fraction from Aconitum coreanum, Carbohyd. Polym. 230 (2020), 115586.

[16] H. Hu, H. Liang, Y. Wu, Isolation, purification and structural characterization of polysaccharide from Acanthopanax brachypus, Carbohyd. Polym. 127 (2015) 94–100.

[17] M. Meng, D. Cheng, L.R. Hang, Y.Y. Chen, C.L. Wang, Isolation, purification, structural analysis and immunostimulatory activity of water-soluble polysaccharides from Grifola Frondosa fruiting body, Carbohyd. Polym. 157 (2017) 1134–1143.

[18] C. Cui, S. Chen, X.Y. Wang, G.W. Yuan, F. Jiang, X.Y. Chen, L. Wang, Characterization of Moringa oleifera roots polysaccharide MRP-1 with anti-inflammatory effect, Int. J. Biol. Macromol. 132 (2019) 844–851.

[19] B. Li, N. Zhang, D.X. Wang, L.L. Jiao, Y. Tan, J. Wang, H. Li, W. Wu, D.C. Jiang, Structural analysis and antioxidant activities of neutral polysaccharide isolated from Epimedium koreanum Nakai, Carbohyd. Polym. 211 (2018) 100–108.

[20] Z,Y. Chen, Y. Zhao, M.K. Zhang, X.F. Yang, P. X. Yue, D.K. Tang, X.L. Wei, Structural characterization and antioxidant activity of a new polysaccharide from Bletilla striata fibrous roots, Carbohyd. Polym. 227 (2020) 115362.

[21] H.K. Jeong, D. Lee, H.P. Kim, S.H. Baek, Structure analysis and antioxidant activities of an amylopectin-type polysaccharide isolated from dried fruits of Terminalia chebula, Carbohyd. Polym. 211 (2019) 100–108.

[22] F. Ginhoux, S. Jung, Monocytes and macrophages: Developmental pathways and tissue homeostasis, Nat. Rev. Immunol. 14 (2014) 392–404.

[23] J.Y. Ren, C.L. Hou, C.C. Shi, Z.H. Lin, W.Z. Liao, E. Yuan, A polysaccharide isolated and purified from Platycladus orientalis (L.) Franco leaves, characterization, bioactivity and its regulation on macrophage polarization, Carbohyd. Polym. 213 (2019) 276–285.

[24] Q. An, X.M. Ye, Y. Han, M. Zhao, S. Chen, X. Liu, X. Li, Z.T. Zhao, Y. Zhang, K.H. Ouyang, W.J. Wang, Structure analysis of polysaccharides purified from Cyclocarya paliurus with DEAE-Cellulose and its antioxidant activity in RAW264.7 cells, Int. J. Biol. Macromol. 157 (2020) 604–615.

[25] Y.J. Liu, K.L. Ge, Z.Q. Yu, X. Li, X.L. Wu, Y. Wang, L. Zhu, W.H. Jin, Y.L. Guo, Activation of NLRP3 inflammasome in RAW 264.7 cells by polysaccharides extracted from Grateloupia livida (Harv.) Yamada, Int. Immunopharmacol. 85 (2020), 106630.

[26] Y.S. Cui, Y.X. Li, S.L. Jiang, A.N. Song, Z. Fu, C.X. Dong, Z. Yao, W. Qiao, Isolation, purification, and structural characterization of polysaccharides from Atractylodis Macrocephalae Rhizoma and their immunostimulatory activity in RAW264.7 cells, Int. J. Biol. Macromol. 163 (2020) 270–278.

[27] V. Piccolo, A. Curina, M. Genua, S. Ghisletti, M. Simonatto, A. Sabò, B. Amati, R. Ostuni, G. Natoli, Opposing macrophage polarization programs show extensive epigenomic and transcriptional cross-talk, Nat. Immunol. 18 (2017) 530–540.

[28] Y.H. Chen, W. Liu, Y.W. Wang, L. Zhang, J. Wei, X.L. Zhang, F.C. He, L.Q. Zhang, Casein kinase 2 interacting protein-1 regulates M1 and M2 inflammatory macrophage polarization, Cell. Signal. 33 (2017) 107–121.

[29] A. Reyes-Díaz, V. Mata-Haro, J. Hernández, A.F. González-Córdova, A. Hernández-Mendoza, R. Reyes-Díaz, M.J. Torres-Llanez, L.M. Beltrán-Barrientos, B. Vallejo-Cordoba, Milk fermented by specific Lactobacillus strains regulates the serum levels of IL-6, TNF-alpha and IL-10 cytokines in a LPS Stimulated murine model, Nutrients 10 (2018) 691.